J Mater Sci (2007) 42:4701–4706
DOI 10.1007/s10853-006-1489-2

Microstructure characterization of in situ synthesized porous Si_3N_4–Si_2N_2O composites using feldspar additive

Rajat Kanti Paul · Chi-Woo Lee · Hai-Doo Kim · Byong-Taek Lee

Received: 5 July 2006 / Accepted: 26 December 2006 / Published online: 26 April 2007

Abstract Porous Si_3N_4–Si_2N_2O bodies fabricated by multi-pass extrusion process were investigated depending on the feldspar addition content (4–8 wt% Si) in the raw silicon powder. The diameter of the continuous pores was about 250 μm. The polycrystalline Si_2N_2O fibers observed in the continuous pores as well as in the matrix regions of the nitrided bodies can increase the filtration efficiency. In the 4 wt% feldspar addition, the diameter of the Si_2N_2O fibers in the continuous pores of the nitrided bodies was about 90–150 nm. A few number of rope typed Si_2N_2O fibers (~4 μm) was found in the case of 8 wt% feldspar addition. However, in the 8 wt% feldspar addition, the matrix showed highly porous structure composed of large number of the Si_2N_2O fibers (~60 nm). The relative densities of the Si_3N_4–Si_2N_2O bodies with 4 wt% and 8 wt% feldspar additions were about 65% and 61%, respectively.

Introduction

For the high temperature applications, silicon nitride (Si_3N_4) ceramic has been received much attractions due to its high mechanical properties, excellent chemical resistance as well as its high thermal property [1–4]. However, it has been recognized that its high production cost was a limiting factor for the fabrication of Si_3N_4 components. On the other hand, the reaction-bonded silicon nitride (RBSN) has been found as promising ceramics because it offers a number of advantages such as using low cost Si powder, the easy control of dimension as well as good thermal stability at high temperatures [5–7].

In addition, Si_2N_2O ceramic showed an excellent oxidation resistance at severe conditions for high temperature engineering purposes [8]. Thus, Si_3N_4–Si_2N_2O composite has been considered as an industrial material because of its superior properties such as high mechanical strength and oxidation resistance [9, 10].

In general, for the densification of Si_3N_4 ceramics, the liquid phase sintering was carried out using different sintering additives such as MgO, Al_2O_3, Y_2O_3, Yb_2O_3 and other rare earth oxides or their combinations [11, 12]. However, to minimize the cost of Si_3N_4–Si_2N_2O composite, the choice of sintering additive with reasonable costs as well as decreasing the sintering temperature are required, especially, for the application of intermediate temperatures. In this point of view, the feldspars, which are aluminosilicates containing different amounts of calcium, potassium, or sodium can be considered as low temperature and low cost sintering additives. In the glass ceramics, the feldspar was widely used as a flux to decrease the vitrifying temperature of ceramics during firing and forming a glassy phase. Thus, the cheaper Si powder and feldspar additives would offer an opportunity to reduce the cost of Si_3N_4–Si_2N_2O composites compared with that of directly sintered Si_3N_4 ceramics using Si_3N_4 powder.

Furthermore, the porous ceramics have been reported as candidate materials as environmental filters for the

R. K. Paul · C.-W. Lee
School of Advanced Materials Engineering,
Kongju National University, 182, Shinkwan-dong, Kongju City,
Chungnam 314-701, South Korea

H.-D. Kim
Ceramic Materials Group, Korea Institute of Machinery
and Materials, Changwon, Kyungnam 641-010, South Korea

B.-T. Lee (✉)
Department of Biomedical Engineering and Materials,
School of Medicine, Soonchunhyang University,
366-1, Ssangyoung-dong, Cheonan-city,
Chungnam 330-090, South Korea
e-mail: lbt@sch.ac.kr

purification systems of polluted air and water [13, 14]. The filtration efficiency can be increased by increasing the surface area of the filter materials. Thus, the filtration efficiency can be increased by the microstructure control of the sintered bodies such as porosity, pore size, pore shape and morphology of the pore surface. Moreover, an introduction of whiskers or fibers on the pore surface can also be an effective method to increase the filtration efficiency due to their high surface area.

In this work, using the feldspar as sintering additive, the continuously porous in-situ Si_3N_4–Si_2N_2O composites were fabricated by multi-pass extrusion process. Especially, the morphology of the Si_2N_2O fibers observed in the porous Si_3N_4–Si_2N_2O composites was investigated depending on feldspar additions.

Experimental procedure

Commercial Silicon (Permascand, Sweden; $d_{50} = 7$ μm, BET = 1.2 m^2/gm) and feldspar (Buyeo Materials, Korea) powders were used as starting materials to make continuously porous Si_3N_4–Si_2N_2O bodies. The feldspar powder contained 75 wt% SiO_2, 14.5 wt% Al_2O_3, 0.1% Fe_2O_3, 0.3 wt% CaO, 6.5 wt% Na_2O, 3.5 wt% K_2O, 0.02 wt% TiO_2, 0.03 wt% MgO and 0.4 wt% MnO.

At first, the silicon powder with different weight percentages of feldspar (2–8 wt%) was ball milled in ethanol and using Si_3N_4 as milling media. After ball milling for 12 h, the dried mixture powder (Si + (2–8 wt%) feldspar), ethylene vinyl acetate (Elvax210 and 250, Dupont, USA) as a binder and stearic acid (CH_3 $(CH_2)_{16}COOH$, Daejung Chemicals & Metals Co., Gyonggi, Korea) as a lubricant were shear mixed homogeneously with a volume ratio of 55/38/7 using a shear mixer (Shina Platec. Co., Suwon, Korea). After shear mixing for 30 min at 120 °C, the homogeneous mixture was extruded through a heated steel die to make filaments with a diameter of 3.5 mm [15]. The extruded filaments were used to produce a tube by warm press. On the other hand, the pore-forming agent carbon (10–15 μm, Aldrich Chemical Co., USA), binder and stearic acid with a volume ratio 48/45/7 were also shear mixed and the mixture was extruded as a rod [16, 17]. To make the core/shell structure of 1st passed filament with a diameter of 3.5 mm, the tube and rod were combined together to prepare the feed roll and extruded at 90 °C as shown in Fig. 1. The 2nd passed filaments were produced by passing the bundle of 1st passed filaments though extrusion.

To remove the binder, a 1st burn-out was employed in a tube furnace at 700 °C in flowing N_2 gas. A 2nd burn-out was carried out at 1000 °C in air for the removal of carbon. To make the continuously porous Si_3N_4–Si_2N_2O ceramics, the nitridation process was performed at 1400 °C in flowing N_2 gas for 20 h.

The phase assemblage of reaction products was identified by X-ray diffraction (CuK_α, D/MAX-250, Rigaku, Japan) technique. The relative density of the nitrided bodies was measured by Archimedes method with an immersion in water. The detailed microstructure, pore size, pore distribution and the morphology of Si_2N_2O fibers of the porous Si_3N_4-Si_2N_2O bodies were observed using field emission scanning electron microscope (JSM-635F, JEOL, Japan) and transmission electron microscope (JEM2010, JEOL) techniques.

Results

Figure 2 shows the SEM images and EDS profiles of raw Si (a) and feldspar (b) powders. The average particle size of the Si powder was almost 7 μm in diameter with irregular shape as shown in Fig. 2c. However, the particle size of feldspar powder was observed in a range of

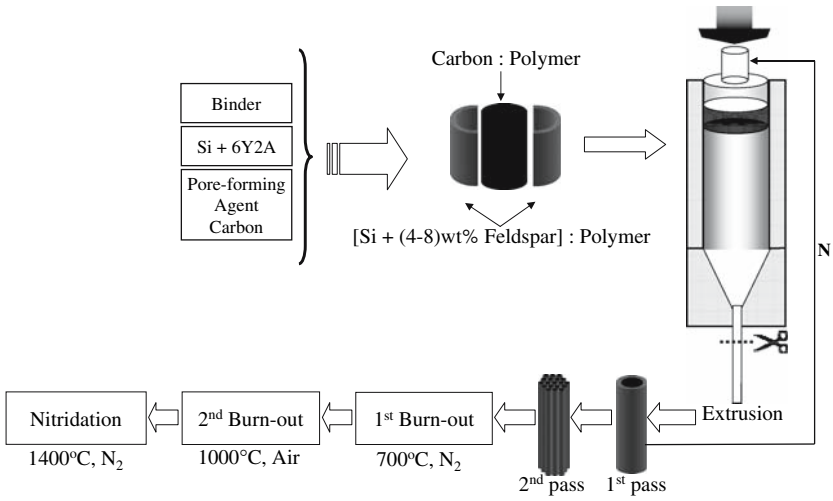

Fig. 1 A schematic diagram of the multi-pass extrusion process

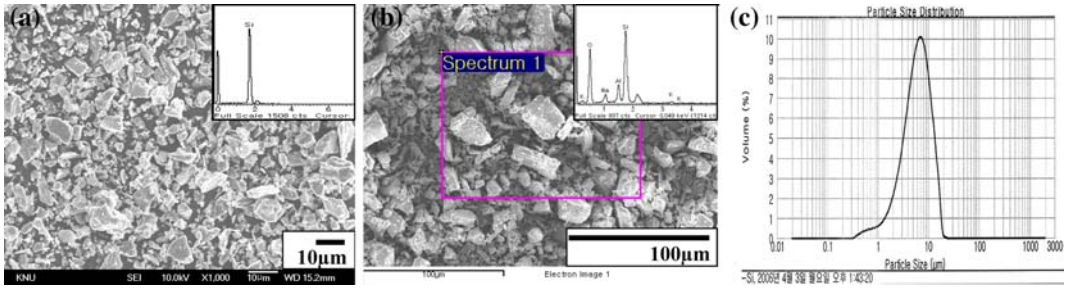

Fig. 2 SEM images and EDS profiles of raw Si (**a**) and feldspar (**b**) powders; (**c**) particle size distribution profile of raw Si powder

2–20 μm in diameter with irregular shape. The inserted EDS profile in Fig. 2(b), in which Si, O, Al, Na and K elements were detected due to the feldspars that contained mainly quartz (SiO_2) and the silicates of aluminum, sodium, potassium, calcium or the combinations of these elements.

Figure 3 shows SEM images of transverse and longitudinal sections of 2nd passed extruded (a, d), 2nd burn-out (b, e) and nitrided (c, f) bodies with 8 wt% feldspar addition. The carbon/polymer (dark contrast) comprised with a pore-forming agent and the Si mixture powder/polymer (comparatively bright contrast) comprised with the matrix in the transverse (a) and longitudinal (d) sections of the extruded body were appeared with an alternate layer. The average diameter of the pore-forming agent was about 260 μm. After 2nd burn-out (b, e), the polymer binder and pore-forming agent were successfully removed to form the continuously porous green body. However, the continuously porous Si_3N_4–Si_2N_2O body (c, f) was produced after nitridation of porous green body at 1400°C in N_2 atmosphere. The diameter of the continuous pores of the nitrided body was slightly decreased with about 240 μm due to the formation of Si_2N_2O fibers on the pore surface which will be clearly observed in Figs. 5 and 6.

Figure 4 shows the XRD profiles of raw Si (a) and feldspar (b) powders, mixture powders of Si–4 wt% feldspar (c), after 2nd burn-out of the extruded body at 1000 °C in air and (d) and nitrided Si_3N_4–Si_2N_2O body at 1400 °C in N_2 atmosphere (e). The feldspar powder (b) was detected with mainly quartz (SiO_2) and Na, Ca-plagioclase together with minor K-feldspars and mica phases. However, in the mixture powders (c), the main peaks were detected with Si and minor phases of quartz and Na,Ca-plagioclase. After 2nd burn-out process (d), the quartz and Na/Ca-plagioclase phases were detected together with Si phase. However, most of the components of the feldspar powder can be changed into an amorphous phase at 1000 °C [18]. On the other hand, in this step, the Si particles can also be oxidized to form SiO_2 film attached on the surfaces. After nitridation at 1400 °C (e), the comparatively strong α-Si_3N_4 peaks were detected together with Si_2N_2O and β-Si_3N_4 phases. The cracks and dislocations in the Si particles which existed during the ball milling process, can enhance the nitridation behavior to form reaction bonded Si_3N_4 during

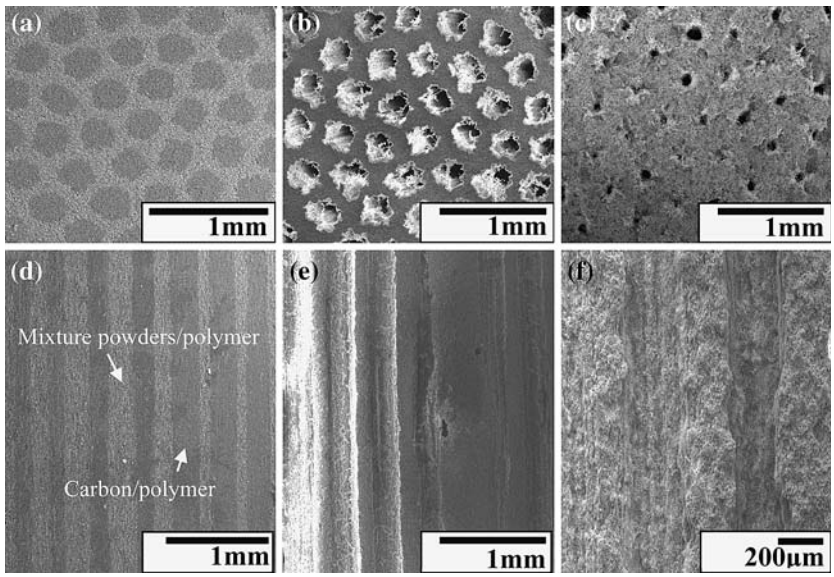

Fig. 3 Low magnification SEM transverse and longitudinal images of the 2nd passed extruded (**a**, **d**), 2nd burn-out (**b**, **e**) and continuously porous Si_3N_4–Si_2N_2O (**c**, **f**) bodies with 8 wt% feldspar addition

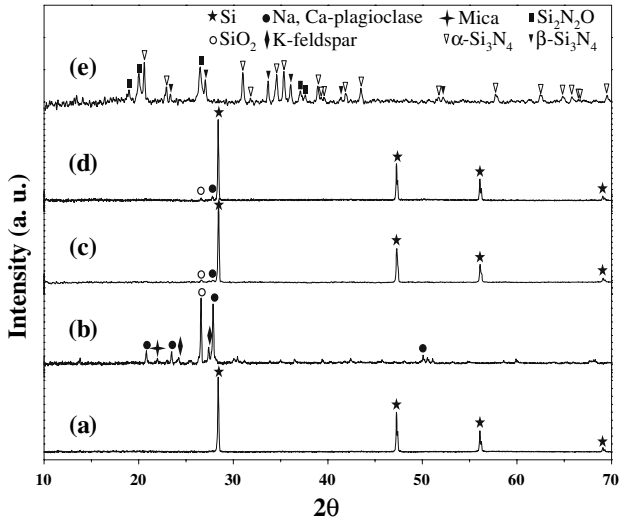

Fig. 4 XRD profiles of (**a**) raw Si powder, (**b**) feldspar powder, (**c**) Si + 4 wt% feldspar powder, (**d**) after 2nd burning-out of the extruded body at 1000 °C in air and (**e**) Si_3N_4–Si_2N_2O body after nitridation at 1400 °C in N_2 atmosphere

nitridation process [5]. However, the formation of Si_2N_2O phase was reported in the phase relation of Si_3N_4–SiO_2–Al_2O_3 or Y_2O_3 systems at high temperature [19, 20].

Figure 5 shows SEM image (a) and enlarged images (b–d) of the continuously porous Si_3N_4–Si_2N_2O bodies with 4 wt% feldspar addition which were taken from the marked P, Q regions in Fig. 5(a) and R region in Fig. 5(c), respectively. In the continuous pores of the nitrided body (b), many Si_2N_2O fibers having 90–150 nm in diameter were observed. The formation of Si_2N_2O fibers was due to the vapor phase reaction between the gaseous intermediate phase SiO and N_2 during the nitridation [21, 22]. This observation was compared with that of Si_2N_2O–Si_3N_4 bodies to which 6Y2A (6 wt% Y_2O_3–2 wt% Al_2O_3) was added as sintering additives. In the case of 6Y2A addition, the network type Si_2N_2O fibers (~50–420 nm in diameter) having high aspect ratio were observed with a smooth and uniform in diameter along their length [23]. On the other hand, the matrix region of the nitrided body (c) also showed micro-channelled microstructure with large number of Si_2N_2O fibers having 70–90 nm in diameter in the micro-pores (d) taken from R region in (c). They can increase the filtration efficiency. However, in this sample, the relative density was about 65%.

Figure 6 shows SEM image (a) and enlarged images (b–d) of the nitrided bodies to which 8 wt% feldspar was added. In this case, the number of Si_2N_2O fibers increased in the continuous pore (b) as well as in matrix (d) regions taken from marked P (a) and R (c) regions because of the increasing of SiO_2 content in the mixture powders due to the increasing content of feldspar. The diameter of the Si_2N_2O fibers in the continuous pore was about 90–150 nm. Some rope typed Si_2N_2O fibers with about 4 μm in diameter were also observed (b). However, in the matrix region (d), the Si_2N_2O fibers were fine (~60 nm in diameter) which were compared with that of 4 wt% feldspar addition, as shown in Fig. 5(d). Also, the matrix region (c) was found with highly porous structure compared with that of the 4 wt% feldspar addition as shown in Fig. 5(c). This was due to the high content of feldspar which was transformed into an amorphous phase during nitridation. In this case, the relative density was decreased to 61% which compared with that of 4 wt% feldspar addition.

Figure 7 shows TEM images of the Si_2N_2O fibers of the continuously porous Si_3N_4–Si_2N_2O bodies nitrided at 1400 °C. In the 4 wt% feldspar addition (a), the Si_2N_2O

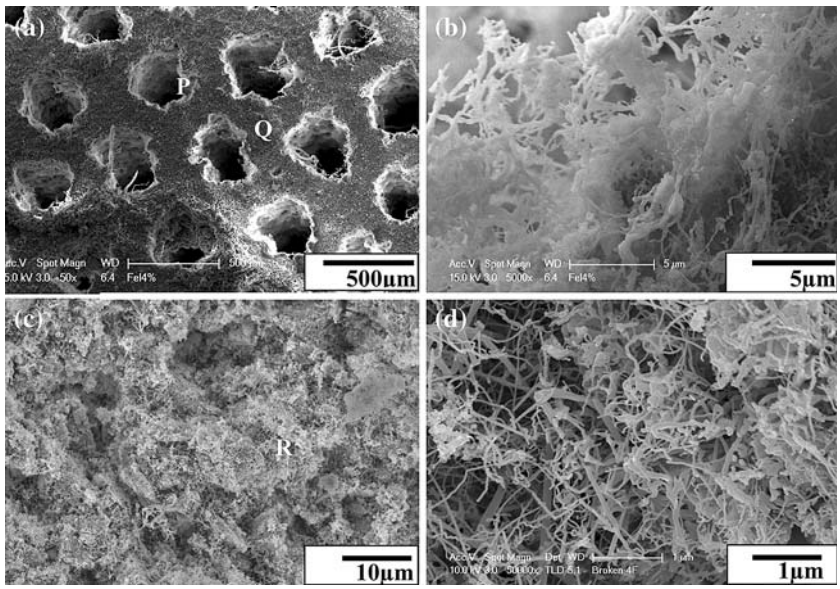

Fig. 5 Low magnification SEM image (**a**) and enlarged images (**b–d**) of the 2nd passed continuously porous Si_3N_4–Si_2N_2O composite with 4 wt% feldspar addition

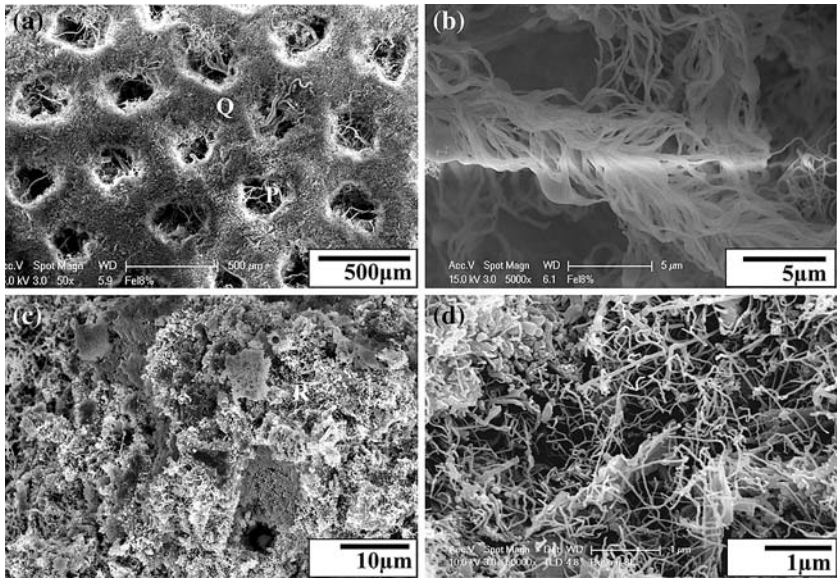

Fig. 6 Low magnification SEM image and enlarged images (**b–d**) of the 2nd passed continuously porous Si_3N_4–Si_2N_2O composite with 8 wt% feldspar addition

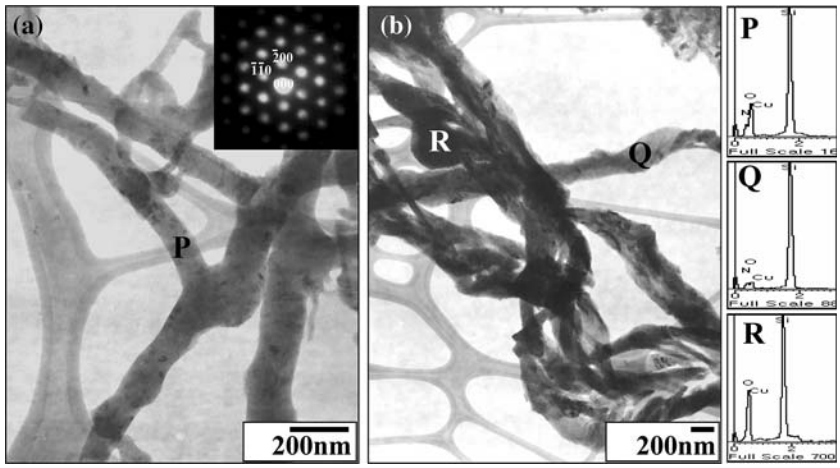

Fig. 7 TEM images and EDS profiles of the Si_2N_2O fibers of the 2nd passed continuously porous Si_3N_4–Si_2N_2O composite; (**a**) 4 wt% feldspar addition and (**b**) 8 wt% feldspar addition

fibers observed in the nitrided bodies were about 90–150 nm in diameter. The inserted diffraction pattern that was taken from the [001] zone axis of P region in (a) and the EDS profile confirmed them as polycrystalline Si_2N_2O. This result was compared with the nitrided bodies with 6Y2A addition in which single crystalline as well as polycrystalline Si_2N_2O fibers were observed [23]. However, in the case of 8 wt% feldspar addition (b), the number of Si_2N_2O fibers which are a part of rope type as shown in Fig. 6(b), were increased due to the increasing amount of SiO_2 in the mixture powder to enhance the formation of Si_2N_2O fibers through the vapor phase reaction. The rope typed Si_2N_2O fibers were confirmed with polycrystalline phase by the analysis of electron diffraction pattern and EDS profiles. The EDS profile taken from the Q region in (b) showed Si_2N_2O phase, but a few droplets also observed on the fibers surface with SiO_2 phase which was confirmed from the EDS profile R taken from the R region in (b). The droplets were formed due to the SiO_2 in the feldspar which was changed into an amorphous phase at high temperature.

Conclusion

Microstructures of porous Si_3N_4–Si_2N_2O composites fabricated by multi-pass extrusion process were investigated depending on feldspar addition. In the continuous pores and the matrix regions, many Si_2N_2O fibers were observed which will be effective to offer high filtration efficiency due to their high surface area. A few numbers of rope type Si_2N_2O fibers was observed in the composites using 8 wt% feldspar addition. In the sample using 4 wt% feldspar addition, the diameter of the fibers found in the continuous pores of the Si_3N_4–Si_2N_2O bodies was about 90–150 nm while in the matrix region was about 90 nm. However, the diameter of the fibers in the continuous pores and matrix

region in the composite using 8 wt% feldspar addition were about 90–150 nm and 60 nm, respectively.

Acknowledgement This work was supported by the ''Center for Environmentally, Friendly Vehicles'' of Eco-Technopia Project.

References

1. Schioler LJ (1985) Am Ceram Soc Bull 64:268
2. Pyzik J, Beaman DR (1993) J Am Ceram Soc 76:2737
3. Riley FL (2000) J Am Ceram Soc 83:245
4. Bressiani JC, Izhevskyi V, Bressiani AHA (1999) Mater Res 2:165
5. Lee BT, Kim HD (1996) Mater Trans JIM 37:1547
6. Lee BT, Yoo JH, Kim HD (2002) Mater Sci Eng A 333:306
7. Lee JS, Mun JH, Han BD, Kim HD, Shin BC, Kim IS (2004) Ceram Intl 30:965
8. Ohashi M, Kanzaki S, Tabata H (1991) J Am Ceram Soc 74:109
9. Emoto H, Mitomo M, Wang CM, Hirosturu H, Inaba T (1998) J Eur Ceram Soc 18:527
10. Radwan M, Kashiwagi T, Miyamoto Y (2003) J Eur Ceram Soc 23:2337
11. Lee BT, Kim HD (2004) Mater Sci Eng A364:126
12. Yamamoto H, Akiyama K, Murakami Y (2006) J Eur Ceram Soc 26:1059
13. Miyakawa N, Sato H, Maeno H, Takahashi H (2003) JSAE Rev 24:269
14. Moreira EA, Innocentini MDM, Coury JR (2004) J Eur Ceram Soc 24:3209
15. Lee BT, Kim KH, Han JK (2004) J Mater Res 19:3234
16. Lee BT, Kang IC, Cho SH, Song HY (2005) J Am Ceram Soc 88:2262
17. Lee BT, Jang DH, Kang IC, Lee CW (2005) J Am Ceram Soc 88:2874
18. Steiner JC, Jahns RH, Luth WC (1975) Geo Soc Am Bull 86:83
19. Mitomo M, Ono S, Asami T, Kang SJL (1989) Ceram Intl 15:345
20. Huag ZK, Greil P, Petzow G (1984) Ceram Intl 10:14
21. Scheffler M, Pippel E, Woltersdorf J, Greil P (2003) Mater Chem Phy 80:565
22. Chollon G, Hany R, Vogt U, Berroth K (1998) J Eur Ceram Soc 18:535
23. Paul RK, Lee CW, Kim HD, Lee BT (2007) Mater Sci Forum 534–536:1049